

# ABSOLUTE SPECTROPHOTOMETRY OF COMET KOHOOTEK 1973f DURING POST-PERHELION PASSAGE

P. S. GORAYA, B. S. RAUTELA, and B. B. SANWAL  
*Uttar Pradesh State Observatory, Manora Peak, Naini Tal, India*

(Received 2 November, 1984)

**Abstract.** Absolute spectrophotometry of the coma of Comet Kohoutek 1973f during post-perihelion period has been presented for seven nights in January 1984. Moderately wide range of heliocentric distance (0.436–0.799 AU) covered during observations allowed us to study the flux variation of emission bands with heliocentric distance. The emission features of CN, CH, C<sub>2</sub>, C<sub>3</sub>, and NaI have been identified in this comet. The abundances of CN and C<sub>2</sub> have been estimated and the production rates of CN, C<sub>2</sub> and C<sub>3</sub> have been derived. Production rates of CN and C<sub>2</sub> seem to vary as  $r^{-0.33}$  and  $r^{-3.50}$  respectively. The continuum of the comet became more and more redder as the heliocentric distance of the comet increased and phase angle decreased.

## 1. Introduction

Comet Kohoutek 1973f provided an excellent and unusual opportunity to investigate different features of cometary bodies. During the recent apparition of Comet Kohoutek, it was of sufficient brightness during the period October 1973 to April 1974 for observations even with small telescopes. Because of all the favourable conditions this comet was observed from a large number of places and has given rise to many new unusual phenomena.

The comet was on perihelion on 28.5 December, 1973 at  $r = 0.20$  AU (Marsden, 1973). It was of maximum brightness,  $m_1 \sim 2.6$  (Angione *et al.*, 1975a) on 4 and 5 January, 1974. But it was much fainter than the predicted brightness ( $m_1 \sim -3.6$ ). After its naked-eye visibility in early January, Comet Kohoutek rapidly faded away afterwards. The broad band infrared observations at  $10 \mu\text{m}$  and  $20 \mu\text{m}$  by Zeilik (1974) showed that the comet was an intense infrared object ( $m_{10 \mu\text{m}} = -4.75$ ,  $m_{20 \mu\text{m}} = -5.70$ ) during 19, 20, and 21 December 1973 ( $r = 0.35$  AU). The light curve (visible estimates of total coma brightness) of Comet Kohoutek has been given by Angione *et al.* (1975a). The objective prism spectrograms of Comet Kohoutek obtained by Miller (1974) on 8 December, 1973, showed the extension of nuclear molecular coma towards antisunward direction. The infrared observations of the comet by Ney (1974) also showed that after perihelion passage the comet possessed an infrared tail and antitail. The continuum energy distribution curves of the comet obtained by Babu (1974a) on 7, 10, and 13 December 1973, showed that the reddening of the scattered light from the head of the comet decreased as the phase angle was increased.

TABLE I  
Basic data of Comet Kohoutek (1973f)

Date (UT) January, 1974	Geocentric distance ( $\Delta$ ) (AU)	Heliocentric distance ( $r$ ) (AU)	$m_1$	Radius of the circular region in the sky at distance $\Delta$ (km) $\times 10^4$	Area of the sky at distance $\Delta$ admitted through the diaphragm (km <sup>2</sup> ) $\times 10^8$
8.56	0.855	0.436	3.99	2.827	25.083
9.55	0.840	0.470	4.07	2.776	24.210
10.56	0.828	0.500	4.13	2.736	23.517
14.58	0.802	0.620	4.34	2.650	22.062
15.57	0.800	0.645	4.41	2.644	21.962
17.56	0.810	0.698	4.57	2.677	22.514
21.58	0.832	0.799	4.98	2.750	23.758

## 2. Observations

The scanner observations of Comet Kohoutek were carried out on seven nights during post-perihelion period. The observations are summarized in Table I. The observations were made with Hilger and Watts monochromator mounted at the 52-cm reflector ( $f/13$ ). The observations were made with the slit set on the nucleus of the coma. The image scale at the focal plane was 30.5 arc sec mm<sup>-1</sup>. A circular diaphragm of 3 mm diameter which corresponds to 91.5 arc sec as projected on the sky, was used for obtaining spectral scans of the comet on all the seven nights. The exit slot of 0.5 mm which corresponds to 33 Å of band pass was used. The instrumentation and observational procedures are same as described earlier (Goraya *et al.*, 1984). Two scans of the comet were secured every night and both scans were averaged. The data points were measured every 25 Å of the entire spectrum. Scans of the neighbouring sky taken before and after each scan of the comet enabled elimination of the contribution by the background sky.

Along with the comet, the standard stars  $\gamma$  Gem and  $\alpha$  CMa were also observed for applying extinction corrections and to be used for calibration purpose. Two late-type stars  $\delta$  Equ (G1V) and 16 Cyg B (G5V) were also used for comparison purpose. The observations of the comet were corrected for atmospheric extinction and were reduced to absolute values with the help of standard stars. The absolute values of the fluxes thus obtained to Tug *et al.* (1977) calibration of  $\alpha$  Lyr. The spectrum scans of the comet reduced to absolute fluxes are shown in Figure 1. Since the observations were made near horizon, so the values of  $\sec z$  vary from 6.3 to 10.3 air mass on 8 January, 1974 and vary as 2.0-6.0 air mass on the remaining nights. Different emission features in Figure 1 are indicated by vertical arrows pointing downwards.

## 3. Radiances of the Emission Bands

The final spectra of Comet Kohoutek are shown in Figure 3. The spectra are shown primarily to identify the various spectral features and to show the night-to-night variations

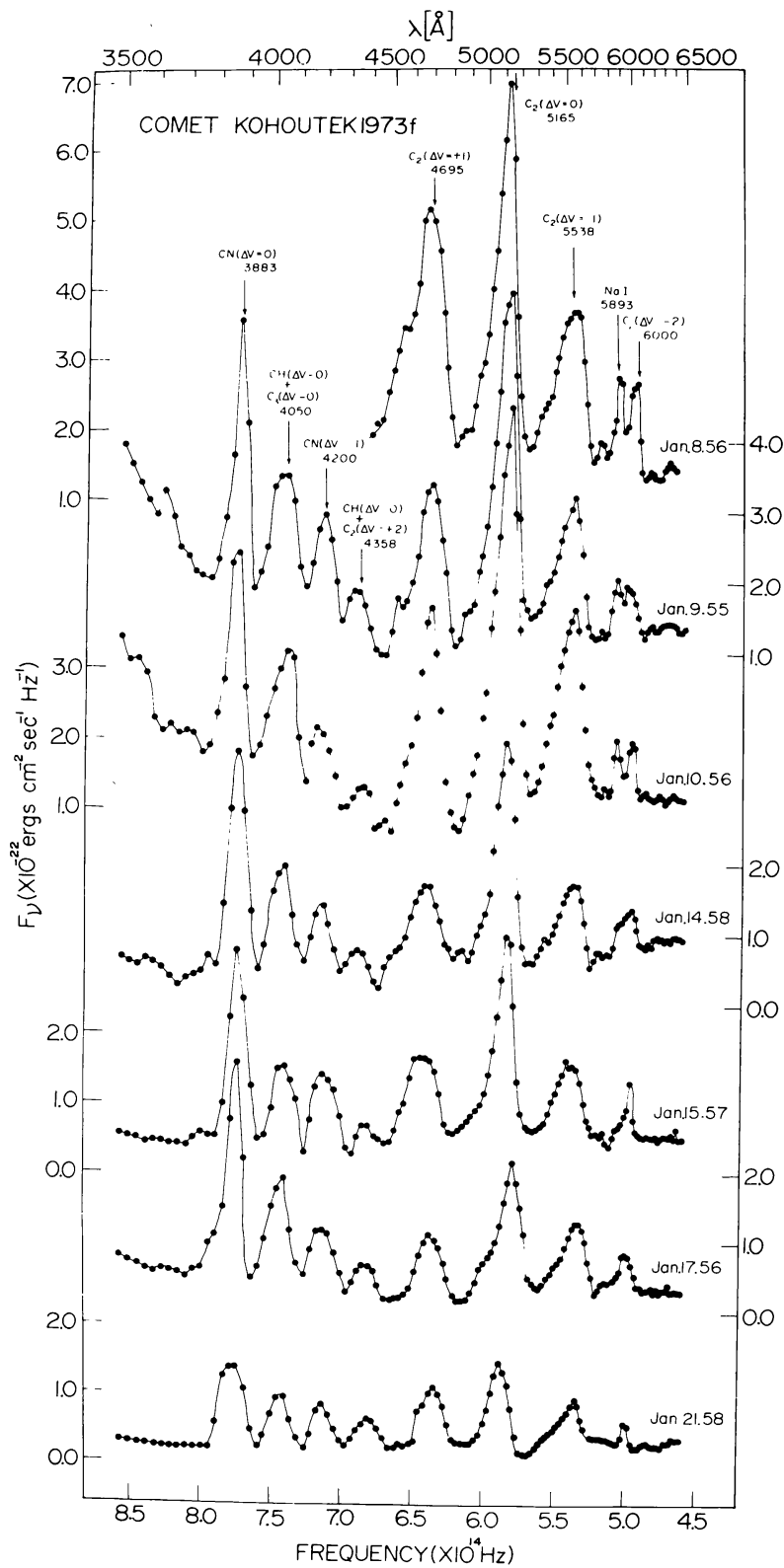


Fig. 1. The absolute flux distribution of the head of Comet Kohoutek 1973f on various dates.

of the strength of the emission bands. A visual examination of these spectra shows several general trends that are of much interest. For example, one can see (by drawing the zero level for each spectrum) that the continuum changes by a factor of 1.6 or more during the observational period. The continuum was strong when the comet was near the Sun. Figure 1 shows the strong emission features of CN ( $\Delta V = 0$ ) and Swan band sequence of  $C_2$  ( $\Delta V = +1, 0$ , and  $-1$ ). The  $C_2$  ( $\Delta V = 0$ ) emission is strongest in all. One can see other emission features of CH +  $C_3$  ( $\Delta V = 0$ ), CN ( $\Delta V = -1$ ), CH ( $\Delta V = 0$ ) +  $C_2$  ( $\Delta V = +2$ ),  $C_2$  ( $\Delta V = -2$ ) and NaI (D-line). NaI emission peak was clearly seen on 8.56, 9.55, and 10.56 January 1974. It started fading onwards, and vanished completely on 21.58 January. It is seen from the Figure that the apparent strength of all emission bands decreases with increasing heliocentric distance. But one can clearly make out that the relative strength of CN emission band increases with increasing heliocentric distance. To know the behaviour of emission strength of different species quantitatively, we have measured the total fluxes of emission bands. In order to measure fluxes in the emission bands, the continuum in the spectrum was located by selecting wavelength regions free of emission lines. The area of the emission bands were measured and converted into the total flux. Since the  $C_2$  ( $\Delta V = 0$ ) band is the strongest, its intensity is easily determined more accurately, we have used it for normalization. The relative fluxes of emission bands normalized with respect to  $C_2$  ( $\Delta V = 0$ ) are given in Table II. The variations of the relative fluxes with heliocentric distance are shown in Figure 2. It is clearly seen in Figure 2 that the relative flux of CN ( $\Delta V = 0$ ) increases rapidly with heliocentric distance. The relative flux of CH +  $C_3$  ( $\Delta V = 0$ ), CN ( $\Delta V = -1$ ) and CH ( $\Delta V = 0$ ) +  $C_2$  ( $\Delta V = +2$ ) increases less rapidly with heliocentric distance, whereas the relative flux of NaI decreases continuously with increasing heliocentric distance. The relative fluxes of  $C_2$  ( $\Delta V = +1$ ),  $C_2$  ( $\Delta V = -1$ ) and  $C_2$  ( $\Delta V = -2$ ) show very slight increase with heliocentric distance. Within observational errors these bands show, more or less, constancy in their fluxes.

In order to show the variation of the observed apparent fluxes of emission bands with heliocentric distance, the observed fluxes were reduced to a standard geocentric distance ( $\Delta = 1.0$  AU). These reduced fluxes ( $\Delta^2 F$ ) for different bands are displayed in Figure 3. Figure 3 reveals that the apparent reduced fluxes of CN ( $\Delta V = 0$ ), CN ( $\Delta V = -1$ ) and CH ( $\Delta V = 0$ ) +  $C_2$  ( $\Delta V = +2$ ) remain almost (only slight decrease) constant as the heliocentric distance increases, whereas the reduced fluxes due to the other emission bands rapidly decrease with increasing heliocentric distance.

#### 4. Number of CN and $C_2$ Molecules

The total number of molecules ( $N$ ) of CN and  $C_2$  contained in a cylinder of diameter 91.5 arcsec in the line of sight and extending through the head of the comet can be computed from the monochromatic fluxes. The total number of molecules contributing to a certain emission band have been computed from the well known relation (cf. O'Dell and Osterbrock, 1962) used in our earlier paper (Goraya *et al.*, 1984). The values of  $f, p$ ,

TABLE II  
Observed fluxes of emission bands relative to  $C_2(\Delta V = 0)$

Date (UT) January, 1974	Apparent flux $F(C_2, \Delta V = 0)$ ( $\text{ergs cm}^{-2} \text{sec}^{-1}$ ) $10^{-9}$	F/F( $C_2, \Delta V = 0$ )		CH( $\Delta V = 0$ ) + $C_2(\Delta V = 0)$ (4050)	CN( $\Delta V = -1$ ) (4200)	CH( $\Delta V = 0$ ) + $C_2(\Delta V = +2)$ (4358)	$C_2(\Delta V = +1)$ (4695)	$C_2(\Delta V = -0)$ (5165)	$C_2(\Delta V = -1)$ (5538)	NaI (5893)	$C_2(\Delta V = -2)$ (6000)	Luminosity (L) $4\pi\Delta^2 F(C_2, \Delta V = 0)$ ( $\text{ergs sec}^{-1}$ ) $\times 10^{18}$
		CN( $\Delta V = 0$ ) (3883)	$C_2(\Delta V = 0)$									
8.56	11.119	-	-	-	-	-	0.675	1.000	0.435	0.089	0.072	22.676
9.55	9.043	0.475	0.356	0.082	0.181	0.082	0.597	1.000	0.509	0.075	0.066	17.805
10.56	10.401	0.408	0.327	0.062	0.137	0.062	0.592	1.000	0.481	0.046	0.046	19.904
14.58	5.064	0.849	0.474	0.126	0.237	0.126	0.636	1.000	0.518	0.071	0.079	9.077
15.57	4.401	0.873	0.450	0.139	0.398	0.139	0.663	1.000	0.509	0.050	0.091	7.856
17.56	3.642	1.153	0.632	0.176	0.384	0.176	0.499	1.000	0.461	0.005	0.060	6.662
21.58	1.668	1.487	0.808	0.237	0.580	0.237	0.719	1.000	0.588	0.000	0.096	3.205

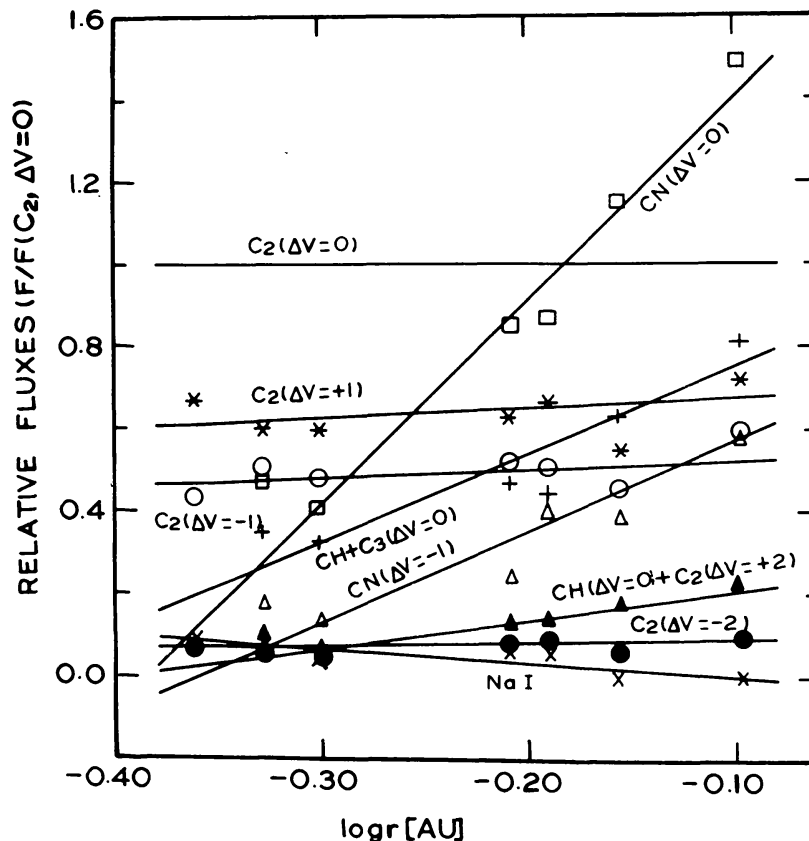


Fig. 2. Variation of the relative fluxes of emission bands as a function of heliocentric distance. The straight lines have been fitted by free hand.

and  $\rho(\nu, r)$  used in our calculations are given in Table III along with their sources. The total number of molecules thus obtained are listed in Table III.

### 5. Production Rates of CN, C<sub>2</sub>, and C<sub>3</sub> Molecules

The molecular production rates ( $Q$ ) are total number of parent molecules evaporated per second. Production rates can be derived from the total luminosity of the respective

TABLE III  
Number of CN and C<sub>2</sub> molecules

Band	$f$	$p$	$\rho(\nu, r)$ (erg cm <sup>-3</sup> )	log N
CN(0-0) $\Delta V = 0$	0.0342 <sup>a</sup>	0.9200 <sup>b</sup>	$4.214 \times 10^{-20} r^{-2b}$	30.408
CN(0-1) $\Delta V = -1$	0.0024 <sup>a</sup>	0.8108 <sup>b</sup>	$6.910 \times 10^{-20} r^{-2b}$	30.946
C <sub>2</sub> (1-0) $\Delta V = +1$	0.0089 <sup>b</sup>	0.2409 <sup>b</sup>	$7.140 \times 10^{-20} r^{-2b}$	31.372
C <sub>2</sub> (0-0) $\Delta V = 0$	0.0239 <sup>a</sup>	0.7335 <sup>b</sup>	$6.445 \times 10^{-20} r^{-2b}$	30.691
C <sub>2</sub> (0-1) $\Delta V = -1$	0.0071 <sup>b</sup>	0.2142 <sup>b</sup>	$8.390 \times 10^{-20} r^{-2b}$	31.321

#### References

- <sup>a</sup> Lambert (1978);  
<sup>b</sup> Goraya *et al.* (1984).

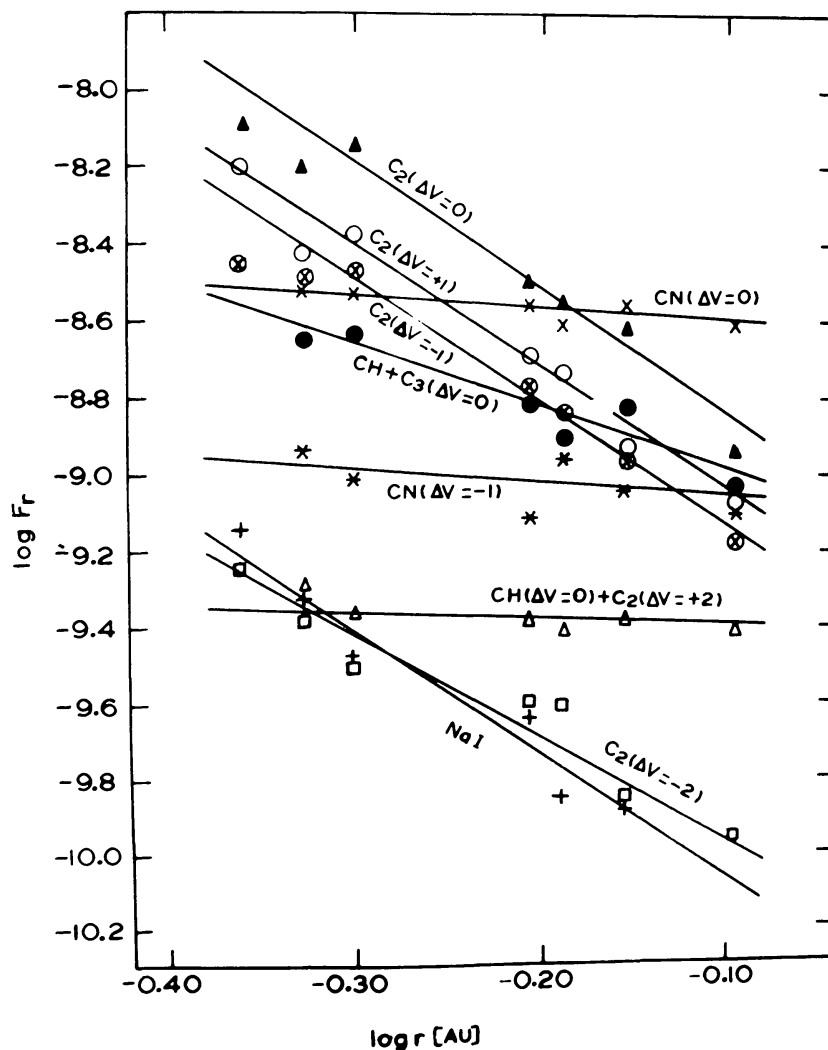


Fig. 3. The reduced fluxes of emission bands as a function of heliocentric distance. The straight lines have been fitted by free hand.

TABLE IV  
Life times and emission rate factors of CN, C<sub>2</sub>, and C<sub>3</sub> species

Species	Emission rate factor (g) <sup>a</sup> photon/sec/mol	Life time <sup>b</sup> (τ) sec	Product (gτ)
CN	$7.42 \times 10^{-2}$	$14.8 \times 10^4$	$1.098 \times 10^4$
C <sub>2</sub>	$4.38 \times 10^{-2}$	$6.6 \times 10^4$	$2.891 \times 10^3$
C <sub>3</sub>	$4.40 \times 10^{-1}$	$4.0 \times 10^4$	$1.760 \times 10^4$

References

<sup>a</sup> Newburn *et al.* (1978);

<sup>b</sup> A'Hearn and Cowan (1975).

molecular band. For deriving the production rates we assume that the only excitation processes responsible in the coma are those induced by solar radiation. Collisions within the coma and excitation by solar wind particles are neglected. For resonance scattering and fluorescence, the luminosity is related to the total number of atoms or molecules,  $N$ , and the emission rate factor  $g$  by the relation (Barth, 1969)

$$L = gN.$$

In terms of life time,  $\tau$ , one have

$$Q = \frac{N}{\tau} = \frac{4\pi\Delta^2 F}{g\tau} = \frac{L}{g\tau}$$

where

$\Delta$  = the comet-earth distance;

$F$  = the observed flux from the comet;

$\tau$  = the life-time of the scattering species; and

$g$  = the probability that a solar photon will be resonantly scattered or produced by resonance fluorescence.

The values of  $g$  and  $\tau$  used in our calculations are given in Table IV along with their sources. The production rates of CN, C<sub>2</sub>, and C<sub>3</sub> molecules are listed in Table V.

As a matter of fact, the life-times are never really observed. They are deduced by dividing the observed scale-length  $S$  by the assumed mean expansion velocity of the molecules. This velocity is probably known to be of the order of 1 or 2 km s<sup>-1</sup>. While  $\tau$  is principally determined by photodestruction process, the product  $g\tau$  is independent of heliocentric distance  $r$  (Feldman *et al.*, 1974), and can conveniently be evaluated at 1 AU. The same procedure has been adopted by us. The  $g$ -factors and life times may be uncertain by as much as  $\pm 50\%$ , producing the same order of uncertainty in production rates. The ratio of the production rate of CN to the production rate of C<sub>2</sub> ( $Q_{\text{CN}}/Q_{\text{C}_2}$ ) is found to vary from 0.08 to 0.27 (as the distance of the comet increases) during observations.

A plot of the variation of production rates of different species with heliocentric distance is shown in Figure 4. A correlation between the total production rates of CN and C<sub>2</sub> is also shown in Figure 5. It is clear from Figure 5 that the production rate of C<sub>2</sub> decreases very rapidly with increasing heliocentric distance, whereas the production rate of CN decreases very slowly with increasing heliocentric distance.

## 6. Continuum Energy Distributions

The continua of comets are not well understood because of the strong emission bands due to cometary molecules. The strong emission bands distort the continuum and make it very difficult to mark its exact location. Optical observations of the continuum radiation from comets can be used to infer the physical properties of solid particles. The wavelength dependence of the scattered light in the optical region is an indicator of the size of the scattering particles.



TABLE V  
Production rates of CN, C<sub>2</sub>, and C<sub>3</sub> molecules

Date (UT) January, 1974	log <i>r</i> (AU)	Production rates of CN, C <sub>2</sub> , and C <sub>3</sub> molecules				log <i>Q</i> (C <sub>3</sub> ) Δ <i>V</i> = 0
		log <i>Q</i> (CN) Δ <i>V</i> = 0	log <i>Q</i> (CN) Δ <i>V</i> = -1	log <i>Q</i> (C <sub>2</sub> ) Δ <i>V</i> = +1	log <i>Q</i> (C <sub>2</sub> ) Δ <i>V</i> = 0	
8.56	-0.361	-	-	27.088	27.198	-
9.55	-0.328	26.191	25.772	26.869	27.093	26.055
10.56	-0.301	26.172	25.697	26.914	27.142	25.915
14.58	-0.208	26.150	25.596	26.604	26.800	25.806
15.57	-0.190	26.099	25.759	26.560	26.738	25.699
17.56	-0.156	26.149	25.672	26.365	26.666	25.696
21.58	-0.098	26.099	25.609	26.208	26.348	25.448
						25.333
						26.120
						26.837
						26.800
						26.823
						26.515
						26.445
						26.330
						25.381
						25.474

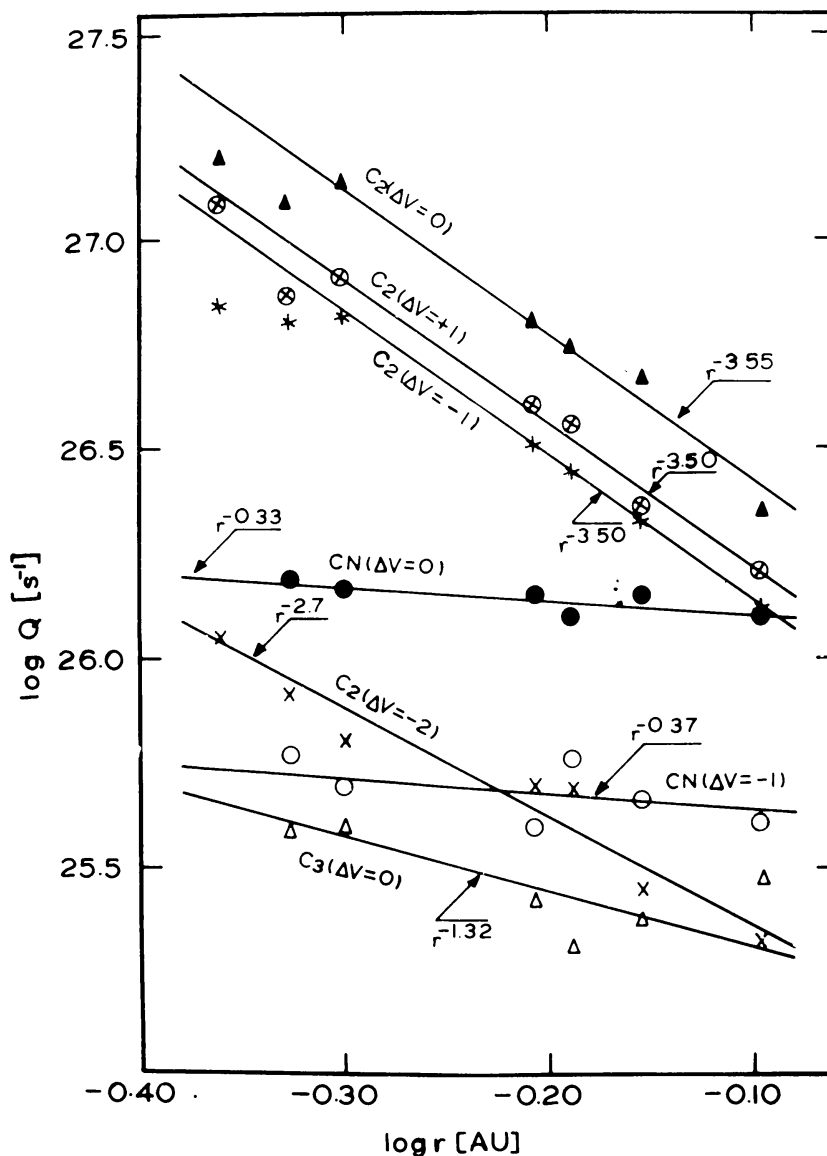


Fig. 4. Variation of the production rates of CN,  $C_2$ , and  $C_3$  species as a function of heliocentric distance. The straight lines have been fitted by free hand.

The colour of the continuum radiation from the coma in the visible part of the spectrum is not clear. In previous studies, some comets were known to have a pure reflection continuum (Gebel, 1970; Ney, 1974; Ney and Merrill, 1976; and Goraya *et al.*, 1982); whereas some comets were found to produce continuum matching with those of the late-type stars around G8 (Bappu and Sinihal, 1960; Vanýsek, 1960; Babu, 1974b; and Kharitonov and Rebristyi, 1974). However, several spectrophotometric studies indicate that the continuum is considerably reddened with respect to the Sun (Liller, 1960; Johnson *et al.*, 1971; Babu and Saxena, 1972; Stokes, 1972; Vanýsek, 1974; Bappu *et al.*, 1980; and Goraya *et al.*, 1984). The continuum was probably due to the scattering of sunlight by solid particles in the comae of those comets.

In an effort to study the continuum of Comet Kohoutek in the present study, the

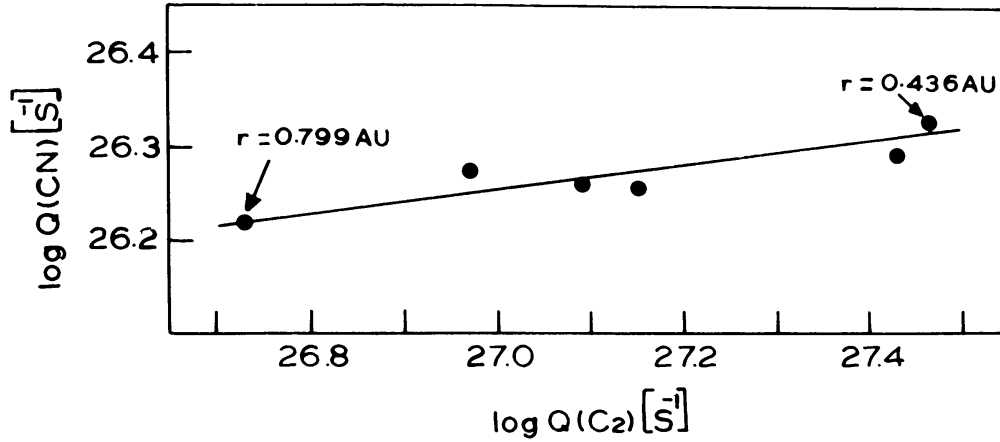


Fig. 5. The correlation between the total production rates of  $\text{C}_2$  and CN molecules. The straight line has been fitted by free hand.

continuum was obtained by taking the line-free regions and using  $\gamma$  Gem and  $\alpha$  CMa as the standard stars. The absolute magnitudes of the continuum normalized to wavelength  $\lambda$  5000 Å are given in Table VI. A plot of these is shown in Figure 6 together with those of Sun and the solar light scattered according to  $\lambda^2$  law (Mie scattering). The energy curves of two late-type stars  $\delta$  Equ (G1V) and 16 Cyg B (G5V) have also been plotted in the same figure for comparison. It is clear from the figure that the continuum of the comet on 8 January resemble well to the reflected continuum of the Sun. On 9 and 10 January the cometary continuum matches, to some extent, with the reflected sunlight. But on 14 and 15 January the cometary continuum matches with that of  $\delta$  Equ (G1V). The continuum of the comet on 17 and 21 January matches well with the continuum of the solar light scattered according to  $\lambda^2$  law.

The most interesting feature to be noted from cometary energy distribution curves in Figure 6 is that they show an increase in reddening with increasing heliocentric distance and decreasing phase angle. Many comets are known to show this type of behaviour (Babu and Saxena, 1972; Vanýsek, 1974; Sivaraman *et al.*, 1979; and Bappu *et al.*, 1980). Babu (1974b) has measured the energy distribution of Comet Kohoutek during pre-perihelion period and has found a decrease in reddening of the continuum with increase in phase angle. The increase in reddening with distance from the Sun can be explained in terms of typical particle sizes. Since some of our continuum measurements, which show this characteristic, can at best be interpreted in terms of optical scattering. We hope that the continuum may be due to the scattering of sunlight by icy particles with rough and porous surfaces of diameters of the order of 0.25 to 5  $\mu\text{m}$ .

The infrared observations of Comet Kohoutek by Ney (1974) between 0.55  $\mu\text{m}$ -18  $\mu\text{m}$  showed that after perihelion passage the coma and tail of the comet have the silicate signature and contain 'black material' (having temperature of  $720 \pm 20$  K). His short-wavelength data showed the spectra of reflected sunlight. He concluded that the coma and tail are composed of small particles of radius  $< 1.1 \mu\text{m}$ . The antitail must be composed of particles of different composition or of large particles of radius  $> 10 \mu\text{m}$ .

TABLE VI

Absolute monochromatic magnitudes of Comet Kohoutek,  $\delta$  Equ, 16 CygB, Sun, and solar radiation scattered according to  $\lambda^2$  law, normalized to  $\lambda$  5000 Å.

Date (UT)	Wavelength (Å)										Name of the object
	3400	3800	4200	4600	5000	5400	5800	6200	6600		
8.56	+ 0 <sup>m</sup> .495	+ 0 <sup>m</sup> .230	+ 0 <sup>m</sup> .060	+ 0 <sup>m</sup> .015	0 <sup>m</sup> .000	+ 0 <sup>m</sup> .065	+ 0 <sup>m</sup> .115	+ 0 <sup>m</sup> .210	+ 0 <sup>m</sup> .320		Comet Kohoutek 1973f
9.55	+ 0.822	+ 0.462	+ 0.225	+ 0.070	0.000	+ 0.015	+ 0.030	+ 0.055	+ 0.106		
10.56	+ 0.930	+ 0.572	+ 0.290	+ 0.091	0.000	- 0.002	+ 0.001	+ 0.020	+ 0.043		
14.58 and 15.57	+ 1.190	+ 0.763	+ 0.380	+ 0.130	0.000	- 0.045	- 0.060	- 0.057	- 0.045		
17.56	+ 1.430	+ 1.020	+ 0.600	+ 0.235	0.000	- 0.100	- 0.160	- 0.215	- 0.278		
21.58	+ 1.550	+ 1.090	+ 0.620	+ 0.200	0.000	- 0.110	- 0.200	- 0.270	- 0.350		
	+ 1.480	+ 0.860	+ 0.350	+ 0.111	0.000	- 0.075	- 0.120	- 0.140	- 0.155		$\delta$ Equ (G1V)
	+ 1.678	+ 1.050	+ 0.470	+ 0.165	0.000	- 0.141	- 0.245	- 0.325	- 0.400		16 Cyg B (G5V)
	+ 0.685	+ 0.340	+ 0.040	- 0.035	0.000	+ 0.065	+ 0.145	+ 0.235	+ 0.340		Sun
	+ 1.520	+ 1.020	+ 0.530	+ 0.190	0.000	- 0.100	- 0.195	- 0.280	- 0.375		Solar radiation scattered according to $\lambda^2$ law.

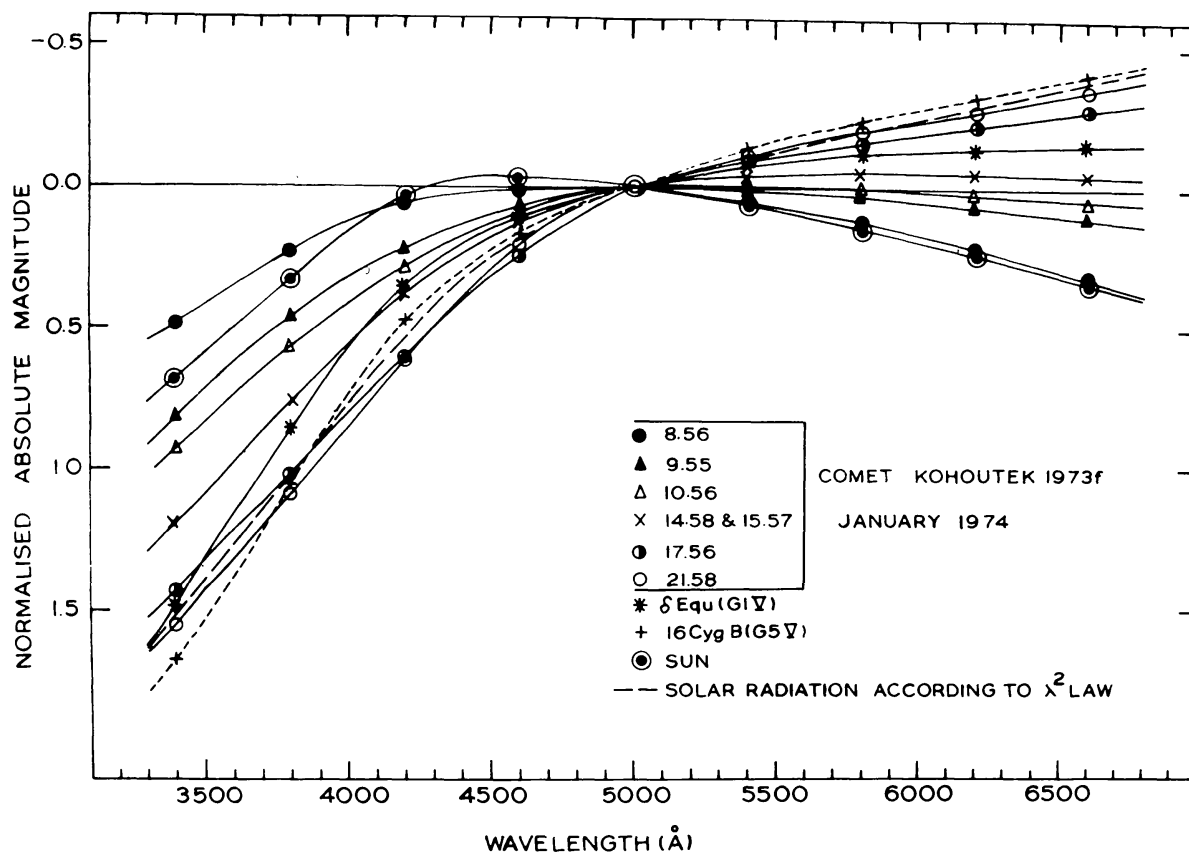


Fig. 6. Continuum energy distributions of Comet Kohoutek 1973f compared with those of  $\delta$  Equ, 16 Cyg B, Sun and solar light scattered according to  $\lambda^2$  law. All curves are normalized to  $\lambda$  5000 Å and the Balmer discontinuity is smoothed out.

Gatley *et al.* (1974) found, from infrared observations of the comet, a thermal component in the coma radiation which has the spectrum of a black body at 440 K (at  $r = 0.43$  AU). The thermal component was also detected by other observers (Noguchi *et al.*, 1974; Zeilik and Wright, 1974) and was attributed to a spherical cloud of dust grains around the nucleus. The grains has radius of  $\sim 1 \mu\text{m}$ . (Noguchi *et al.*, 1974).

## 7. Discussion

The variations of fluxes of emission bands with heliocentric distance are shown in Figures 2 and 3. As customarily the relative flux of CN increases with increasing heliocentric distance. The measurements of fluxes of CN and  $C_2$  bands by Angione *et al.* (1975b) in December 1973 and January 1974 show that the CN and  $C_2$  emission appear to be stronger after perihelion. Neff *et al.* (1976) and Bouška *et al.* (1977) have derived the number of CN and  $C_2$  molecules from absolute spectrophotometry of Comet Kohoutek. Their values of numbers of CN and  $C_2$  molecules agree with ours. Bouška *et al.* (1977) have found that the total number of CN molecules were somewhat larger than before the perihelion passage of the comet than after the perihelion passage. The same behaviour was

found for  $C_2$  molecules. A'Hearn and Cowan (1975) have derived the production rate of CN and  $C_2$  molecules and have shown their variation with heliocentric distance ( $\log Q(\text{CN})$  varies as  $r^{-4}$  and  $\log Q(C_2)$  varies as  $r^{-3.5}$ ). For  $C_2$  molecules our results agree with their findings but for CN molecules our results differ too much from their results as is shown in Figure 4 ( $\log Q(\text{CN})$  varies as  $r^{-0.35}$ ).

The infrared observations of Comet Kohoutek by Ney (1974) showed that after perihelion passage the comet possessed an infrared tail and antitail. Perhaps the most remarkable result of Comet Kohoutek is the extension of nuclear molecular (CN and  $C_2$ ) coma towards antisunward direction (upto distances of  $10^6$  km) as reported by Miller (1974). Such pronounced antisunward elongation of neutral molecular coma is unusual. This contrasts with the normally almost circular CN and  $C_2$  comae observed in earlier comets.

Probably the most important feature in cometary study is the Sodium (NaI) emission. The sodium emission was very well seen in Comet Kohoutek. Sodium emission was strong in the pre-perihelion spectra but weak in the post-perihelion ones (Bappu *et al.*, 1974 and A'Hearn, 1975). A'Hearn (1975) and Kohoutek and Rahe (1975) reported that the sodium D-lines were strong in early January but 'almost vanished' on 12 January, 1974. But Bappu *et al.* (1974) reported that in the pre-perihelion period D-line emission was first noticed on 9 December, 1973, when the comet was at  $x = 0.67$  AU and at a heliocentric latitude of  $\theta = 21^\circ 17'$ . In the post-perihelion period the spectrum of 14 January 1974 showed strong D-line emission. Lee and Skoza (1974) reported that on 16 January 1974, D-line emission was faintly seen. They concluded that the D-line emission should have vanished on the 17th. Bappu *et al.* (1974) indirectly confirmed this with their photographs of the gas tail of Comet Kohoutek. Our spectrum scans (Figure 1) of Comet Kohoutek show that sodium emission was present on 8, 9, 10, 14, and 15 January 1974. But the sodium emission was found absent on 17 January 1974 which is in agreement with the results of Bappu *et al.* (1974). The sodium was also found absent on 21 January, 1974. The heliocentric distance of the comet on 17 January, 1974 was  $r = 0.67$  AU and heliocentric latitude was  $\theta = 6^\circ 50'$ . This agrees very well with the earlier studies on the D-line emission in comets (c.f. Bappu and Sivaraman, 1969).

### Acknowledgement

The authors are thankful to Mr. G. S. D. Babu for help in observations.

### References

- A'Hearn, M. F.: 1975, *Astron. J.* **80**, 861.  
 A'Hearn, M. F.: and Cowan, J. J.: 1975, *Astron. J.* **80**, 852.  
 Angione, R. J., Gates, B., Henize, K. G., and Roosen, R. G.: 1975a, *Icarus* **24**, 111.  
 Angione, R. J., Roosen, R. G., and Lanning, H.: 1975b, *Icarus* **24**, 116.  
 Babu, G. S. D.: 1974a, *Bull. Astron. Soc. India* **2**, 35.  
 Babu, G. S. D.: 1974b, 'The study of Comets', in Donn *et al.* (eds.), *Proc. IAU Coll. No. 25*, p. 220.  
 Babu, G. S. D. and Saxena, P. P.: 1972, *Bull. Astron. Inst. Czech.* **23**, 348.  
 Bappu, M. K. V. and Sinval, S. D.: 1960, *Monthly Notices Roy. Astron. Soc.* **120**, 152.

- Bappu, M. K. V. and Sivaraman, K. R.: 1969, *Solar Physics* **10**, 496.
- Bappu, M. K. V., Parthasarathy, M., and Sivaraman, K. R.: 1974, *Bull. Astron. Soc. India* **2**, 35.
- Bappu, M. K. V., Parthasarathy, M., Sivaraman, K. R., and Babu, G. S. D.: 1980, *Monthly Notices Roy. Astron. Soc.* **192**, 641.
- Barth, C. A.: 1969, *Appl. Opt.* **8**, 1295.
- Bouška, J., Mrkos, A., and Müllerová, E.: 1977, *Bull. Astron. Inst. Czech.* **28**, 288.
- Feldman, P. D., Takacs, P. Z., and Fastie, W. G.: 1974, *Science* **185**, 705.
- Gatley, I., Becklin, E. E., Neugebauer, G., and Werner, M. W.: 1974, *Icarus* **23**, 561.
- Gebel, W. L.: 1970, *Astrophys. J.* **161**, 765.
- Goraya, P. S., Sinha, B. K., Chaubey, U. S., and Sanwal, B. B.: 1982, *The Moon and the Planets* **26**, 3.
- Goraya, P. S., Rautela, B. S., and Sanwal, B. B.: 1984, *Earth Moon, and Planets* **30**, 63.
- Johnson, T. V., Lebofsky, L. A., and McCord, T. B.: 1971, *Publ. Astron. Soc. Pacific.* **83**, 93.
- Kharitonov, A. V. and Rebristyi, V. T.: 1974, *Sov. Astron.* **17**, 672.
- Kohoutek, L. and Rahe, J.: 1974, 'The Study of Comets', in B. Donn *et al.* (eds.), *Proc. IAU Coll.* No. 25, p. 159.
- Lambert, D.: 1978, *Monthly Notices Roy. Astron. Soc.* **182**, 249.
- Lee, P. and Skoza, D.: 1974, *IAU Cir.* No. 2623.
- Liller, W.: 1960, *Astrophys. J.* **132**, 867.
- Marsden, B. G.: 1973, *IAU Cir.* No. 2577.
- Miller, F. D.: 1974, *Publ. Astron. Soc. Pacific.* **86**, 1001.
- Neff, J. S., Ketelsen, D., and Schmidt, G. D.: 1976, *Icarus* **27**, 545.
- Ney, E. P.: 1974, *Astrophys. J.* **189**, L141.
- Ney, E. P. and Merrill, K. M.: 1976, *Science* **194**, 1051.
- Newburn, R. L., J. R., and Johnson, T. V.: 1978, *Icarus* **35**, 360.
- Noguchi, K., Sato, S., Maihara, T., Okuda, H., and Uyama, K.: 1974, *Icarus* **23**, 545.
- O'Dell, C. R. and Osterbrock, D. E.: 1962, *Astrophys. J.* **136**, 559.
- Sivaraman, K. R., Babu, G. S. D., Bappu, M. K. V., and Parthasarathy, M.: 1979, *Monthly Notices Roy. Astron. Soc.* **189**, 897.
- Stokes, G. M.: 1972, *Astrophys. J.* **177**, 829.
- Tug, H., White, N. M., and Lockwood, G. W.: 1977, *Astron. Astrophys.* **61**, 679.
- Vanýsek, V.: 1960, *Bull. Astron. Inst. Czech.* **11**, 215.
- Vanýsek, V.: 1974, 'The Study of Comets', in B. Donn, *et al.* (eds.), *Proc. IAU Coll.* No. 25, p. 1.
- Zeilik, M.: 1974, *Nature* **248**, 120.
- Zeilik, M. and Wright, E. L.: 1974, *Icarus* **23**, 577.